Advanced Synthesis & Catalysis

Accepted Article

Title: Computationally-led Ligand Modification using Interplay between Theory and Experiments: Highly Active Chiral Rhodium Catalyst Controlled by Electronic Effects and CH–π Interactions

Authors: Toshinobu Korenaga, Ryo Sasaki, Toshihide Takemoto, Toshihisa Yasuda, and Masahito Watanabe

This manuscript has been accepted after peer review and appears as an Accepted Article online prior to editing, proofing, and formal publication of the final Version of Record (VoR). This work is currently citable by using the Digital Object Identifier (DOI) given below. The VoR will be published online in Early View as soon as possible and may be different to this Accepted Article as a result of editing. Readers should obtain the VoR from the journal website shown below when it is published to ensure accuracy of information. The authors are responsible for the content of this Accepted Article.

To be cited as: *Adv. Synth. Catal.* 10.1002/adsc.201701191

Link to VoR: http://dx.doi.org/10.1002/adsc.201701191

10.1002/adsc.201701191

FULL PAPER

DOI: 10.1002/adsc.201((will be filled in by the editorial staff))

Computationally-led Ligand Modification using Interplay between Theory and Experiments: Highly Active Chiral Rhodium Catalyst Controlled by Electronic Effects and CH–π Interactions

Toshinobu Korenaga,[a,*] Ryo Sasaki,[a] Toshihide Takemoto,[b] Toshihisa Yasuda,[b] Masahito Watanabe[b]

[a] Department of Chemistry and Biological Sciences, Faculty of Science and Engineering, Iwate University, 4-3-5 Ueda, Morioka, Iwate 020-8551, Japan
E-mail: korenaga@iwate-u.ac.jp
[b] Central Research Laboratory, Technology and Development Division, Kanto Chemical Co., Inc., Soka, Saitama 340-0003, Japan

Received: ((will be filled in by the editorial staff))

Supporting information for this article is available on the WWW under http://dx.doi.org/10.1002/adsc.201######.((Please delete if not appropriate))

Abstract. A chiral ligand for the rhodium-catalyzed asymmetric 1,4-addition of arylboronic acid to a coumarin substrate that could markedly reduce catalyst loading was developed using interplay between theoretical and experimental approaches. Evaluation of the transition states for insertion and for hydrolysis of intermediate complexes (which were emphasized in response to the experimental results) using DFT calculations at the B97D/6-31G(d) with the LANL2DZ basis set for rhodium revealed that: a) the electron-poor nature of the ligands; and b) CH–π interactions between the ligand and coumarin substrates played significant roles in both acceleration of insertion and inhibition of $ArB(OH)_2$ decomposition (protodeboronation). The computationally-designed ligand, incorporating above information, decreased the catalyst loading up to 0.025 mol% (S/C = 4,000), which is less than one one-hundredth relative to past catalyst loadings of typically 3 mol%, with almost complete enantioselectivity. Furthermore, the gram-scale synthesis of the urological drug, (*R*)-Tolterodine (*L*)-tartrate, was demonstrated without the need of intermediary purification.

Keywords: Asymmetric 1,4-addition; DFT calculations; Transition states; Chiral phosphine ligand; Pharmaceutical molecule

Introduction

The development of an efficient catalytic reaction requires many screenings of existing catalysts or many tests of modified catalysts for activity. When the modification or a *de novo* design of a catalyst is attempted, success will depend on a chemist's intuition as well as knowledge, experience, and the experimental results. Computational chemistry could aid in these approaches,[1] but a computationally-led design for the development of effective catalysts is not commonplace because: a) specialized skills are required to carry out the necessary calculations correctly and b) sufficiently accurate calculations are not always affordable.[2] This is particularly the case in organometallic systems which are very complicated due to the complex and multistep catalytic cycles.[3] Furthermore, because compromises of a calculation method are necessary at present, it is important to validate the calculation results by comparison with reference data.[2b,4] Recently, the interplay between theoretical and experimental approaches has been reported to contain profound insight into catalytic reactions, including transition metal catalysts.[5,6] This interplay method has the potential for reactivity prediction of catalytic reactions because it can be performed with computationally-deep considerations of the catalytic cycle, including transition states based on experimental results. Therefore, the method would enable computationally-led rational design of the catalyst for improving catalytic activity or selectivity. In particular, some successful examples of improvement of stereoselectivity by computationally-led design of catalysts were reported.[1,7] In contrast, only a few results have been reported for the improvement of catalytic activity using computational ligand design with this interplay method. Schoenebeck designed and synthesized bisphophines-bearing CF_3 groups to enhance the reductive elimination of Ph-CF_3 from palladium, although that in itself was not the catalytic reaction.[8] Yoshizawa and Nishibayashi demonstrated activity improvement of a molybdenum catalyst for ammonia synthesis using the interplay method.[9] Introduction of electron-donating methoxy groups to a ligand designed by calculations accelerated the molybdenum-catalyzed nitrogen fixation to give ca. 1.5 times the amount of ammonia. Anderson and Straker et al. reported excellent computational ligand design.[10] They developed a highly reactive rhodium catalyst for the enantioselective and

Accepted Manuscript

This article is protected by copyright. All rights reserved.

diastereoselective cycloisomerization of ynamide-vinylcyclopropanes to [5.3.0]-azabicycles. The computationally-designed ligand, bearing fluorine groups, improved the reaction time (e.g., 1 h → 5 min) and enantioselectivity of the catalytic reaction. The above examples show that the interplay method is very useful for rational catalyst design, but the examples, thus far, have not yet used the interplay method to reduce catalyst loadings. Therefore, we will use the interplay method to develop the ligand for practically usable catalyst at scales viable for the pharmaceutical industry.

We were interested in rhodium-catalyzed asymmetric 1,4-addition of arylboronic acids to enone substrates (the so-called Hayashi–Miyaura coupling)[11,12] because the C-C bond formation reaction produces chiral 1,4-adducts (**1**), which include many useful chiral synthetic intermediates.[13] Even though many effective chiral rhodium catalysts for the reaction have been developed, it is hard to utilize the reaction for industrial scale syntheses.[14] Although some examples of gram or kilogram scale reactions have been reported, the catalyst loading was over 1 mol% in all cases.[14,15] Because a rhodium complex is very expensive, the large amount of rhodium complex typically required does not justify the cost in industrial synthesis. The rhodium-catalyzed asymmetric 1,4-addition to 6-methylcoumarin (**2a**) with phenylboronic acid (**3a**) is a typical example of an unfavorable reaction for industrial scale use. The reaction gives (*R*)-6-methyl-4-phenylchroman-2-one (**1aa**), which can be converted readily to Detrusitol® ((*R*)-tolterodine (*L*)-tartrate), an important urological drug (Scheme 1).[16] Since the reaction using rhodium/(*R*)-SEGPHOS catalyst was demonstrated by Hayashi,[17] the same reaction was reported by us using the rhodium/(*R*)-MeO-F_{12}-BIPHEP catalyst,[18] by Carnell using a rhodium/chiral diene ligand,[19] and by Mino using the rhodium/(*R*)-BICMAP (2,2'-diphenylphosphino-1,1'-bi-5,6-dihydrobenzofuran) catalyst.[20] Although the reactions gave (*R*)-**1aa** in high yield with high enantioselectivity, over 99% ee, the catalyst loadings were 3 to 6 mol% (S/C = 33 to 17) in all above examples. Similar examples using coumarin (**2b**) instead of **2a** also required high catalyst loadings.[17-20,21,22] Furthermore, the typically required amount of **3a** is 10 equivalents because consumption of **3a** by protodeboronation[12c] arises from the low reactivity of **2a**.

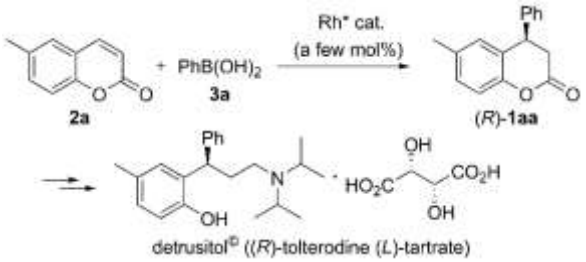

Scheme 1. Synthesis of Detrusitol® via rhodium-catalyzed asymmetric 1,4-addition of **3a** to **2a**.

This work demonstrates development of a chiral rhodium catalyst to drastically reduce the catalyst loading to 0.025 mol% (S/C = 4,000) in the asymmetric 1,4-adddition of **3a** to coumarins **2** by computationally-led chiral ligand design using the interplay between theoretical and experimental approaches. Furthermore, a synthetic protocol for (*R*)-tolterodine synthesis from (*R*)-**1aa** is also demonstrated to utilize the industrial synthesis.[23]

Results and Discussion

Firstly, chiral ligands were screened for asymmetric 1,4-addition of **3a** to **2a** in the presence of 0.1 mol% rhodium catalyst (S/C = 1000). The reactions of **2a** with 1 equiv. of **3a** were performed in 1,4-dioxane, which was a typical solvent for the reaction, with aqueous solution of $NaHCO_3$ at 25 °C for 6 h using known chiral ligands for rhodium (rhodium/ligand = 1.0) (Table 1). Conventional chiral ligands (BINAP, SEGPHOS, and MeO-BIPHEP) were useless for the 1,4-addition reaction (entries 2-4). The electron-poor difluorphos[24] and chiral diene ligands were also not effective (entries 5 and 1). When highly electron-poor MeO-F_{12}-BIPHEP was used, the reaction proceeded to give (*R*)-**1aa** in 23% yield with >99% ee (entry 6). However, the use of even more electron-poor MeO-3,5-$(CF_3)_2$-BIPHEP decreased the yield of (*R*)-**1aa** to 8% and with an inadequate enantioselectivity of 92% ee (entry 9). The results indicated that the electron-poor nature of the chiral diphosphine is important for enhancing the catalytic activity of rhodium,[25] but that is not enough as a requirement for the 1,4-addition reaction to progress. Next, we focused on both the yields and the residual quantity of **3a** (Table 1). A certain amount of **3a** was always consumed regardless if the ligands were ineffective at catalyzing the 1,4 addition (entries 1–5).[12c] The consumption of **3a** was further accelerated using highly electron-poor phosphines. Although the reaction using MeO-F_{12}-BIPHEP or MeO-3,5-$(CF_3)_2$-BIPHEP gave only low yields of the 1,4-addition product, (*R*)-**1aa**, no residual **3a** was observed in the reaction solution (entries 6 and 9). These results revealed that the reason for incomplete 1,4-addition was not only the low catalytic activity of the rhodium/diphosphine system, but also the disappearance of reagent **3a**. However, increasing amount of **3a** to 3.5 equiv. improved the yield to only 38% (entry 7). Furthermore, increasing reaction temperature to 50°C accelerated decomposition of **3a** and gave no product of (*R*)-**1aa** (entry 8). Therefore, further improvement proved difficult using the known ligands.

Table 1. Ligand Screening for Rhodium-catalyzed Asymmetric 1,4-Addition of **3a** to **2a** (S/C = 1,000) [a]

Accepted Manuscript

This article is protected by copyright. All rights reserved.

10.1002/adsc.201701191

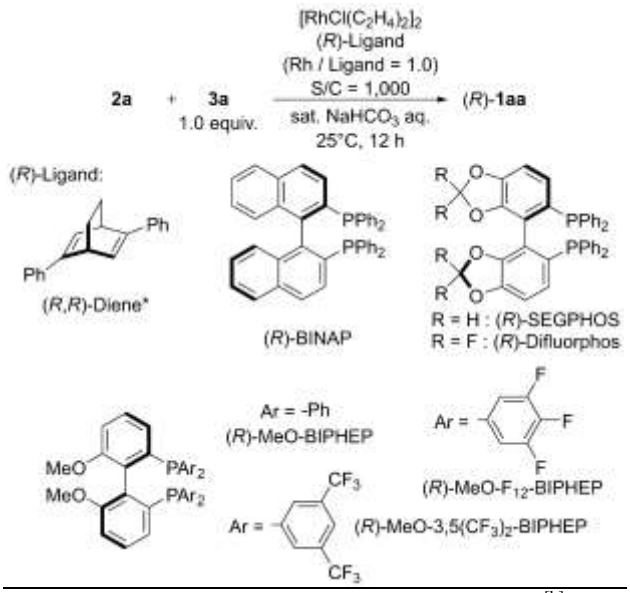

Entry	(*R*)-Ligand	Yield [%]	*ee* [%]	**3a**[b]
1	diene*	1	-	ca. 80%
2	BINAP	0	-	ca. 80%
3	SEGPHOS	0	-	ca. 50%
4	MeO-BIPHEP	0	-	ca. 50%
5	difluorphos	0	-	ca. 90%
6	MeO-F_{12}-BIPHEP	23	>99	none
7[c]	MeO-F_{12}-BIPHEP	38	>99	none
8[d]	MeO-F_{12}-BIPHEP	0	-	none
9	MeO-3,5-$(CF_3)_2$-BIPHEP	8	92	none

[a]Reaction conditions: **2a** (4.32 mmol), $[RhCl(C_2H_4)_2]_2$ (2.16 μmol, 0.1 mol% of Rh), (*R*)-ligand (4.32 μmol, 0.1 mol%), $PhB(OH)_2$ (4.32 mmol, 1.0 equiv.) and sat. $NaHCO_3$ (5.8 mL) in 1,4-dioxane (4.3 mL) under argon atmosphere at 25 °C for 6 h, unless otherwise specified. [b]Remaining quantity of **3a** was calculated by ^1H NMR. [c]$PhB(OH)_2$ (15.1 mmol, 3.5 equiv.). [d]At 50 °C.

Although abnormal consumption of **3a** in Hayashi–Miyaura coupling is known as protodeboronation of the arylboronic acid,[12c] it was evident that this was not simply hydrolysis of **3a** with H_2O because the abnormal consumption of **3a** was not observed in the reaction with a highly reactive cyclohexenone substrate.[26] Therefore, we had an insight into the catalytic cycle of the asymmetric 1,4-addition of **3a** to **2a** according to the catalytic cycle proposed by Hayashi et al.[27] (Figure 1). The active species of $[RhOH(ligand)]_2$ **4**, which is generated from $[RhCl(ligand)]_2$ with base and H_2O, undergoes transmetalation with **3a** to give complex **5**. The insertion reaction of **5** coordinated with **2a** (**5•••2a**) forms the C-C bond asymmetrically. The hydrolysis of complex **6** gives (*R*)-**1aa** and regenerates the active species **4** in dimer form (**4•••4**). The low-reactivity of **2a** slows the reaction rate of insertion (k^{ins}), resulting in a change of the rate-determining step to insertion,[28] while hydrolysis of complex **5** is actualized ($k^{ins} < k^{hyd}$) to enhance the consumption of **3a**, unlike the reaction of cyclohexenone instead of **2a**. If the insertion reaction can be accelerated by an appropriate ligand, the reaction rate of insertion (k^{ins}) would be enhanced and the hydrolysis of complex **5** (k^{hyd}) will be disturbed. However, finding the appropriate chiral ligand using random or intuitive screenings has limitations, as shown in Table 1. Therefore, the rational design of a ligand is essential for accelerating this catalytic reaction.

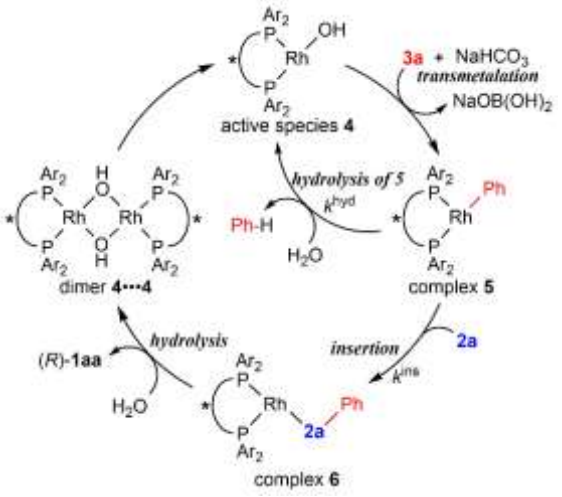

Figure 1. Catalytic cycle of rhodium-catalyzed asymmetric 1,4-addition of **3a** to **2a**.

To design the effective ligand, the insertion step and hydrolysis of **5** were estimated by density functional theory (DFT) calculations. Although some theoretical consideration of enantioselectivity in rhodium-catalyzed asymmetric 1,4-addtion were reported,[29] there are few reports evaluating the catalytic reaction rate by theoretical calculations.[30] Furthermore no examples were reported for hydrolysis of intermediate Rh-Ph complex **5**.

All structures, including transition states, were fully optimized and characterized using frequency calculations at the B97D functional[31] with the 6-31G(d) basis set[32] for the organic molecules and the LanL2DZ[32] basis set (with effective core potentials) for rhodium using Gaussian 09, revision E.01.[33] The B97D functional was chosen by the results of comparison with other functions (B3LYP and M062X: See Supporting Information). Gibbs free energies (298.15 K, 1 atm) were initially computed for the gas phase. Relative Gibbs free energies in solvent were obtained using single-point energy calculations of the optimized structures at the same level with the SCRF method based on CPCM (1,4-dioxane)[34] followed by the addition of thermal corrections, which were calculated using the

Accepted Manuscript

This article is protected by copyright. All rights reserved.

geometrical optimization mentioned above. As the initial calculation structures of Rh/MeO-F_{12}-BIPHEP complexes, a partial X-ray structure of [RhCl(meo-f_{12}-biphep)]$_2$ was used.[26a]

The energy diagrams for both the insertion of **2a** to complex **5**, giving the (*R*)-product as a favorable enantiomer,[35] and the hydrolysis of complex **5**, i.e., decomposition process of **3a**, are summarized in Figure 2. The models used existing chiral ligands: (*R*)-MeO-F_{12}-BIPHEP (black) or (*R*)-MeO-BIPHEP (blue).

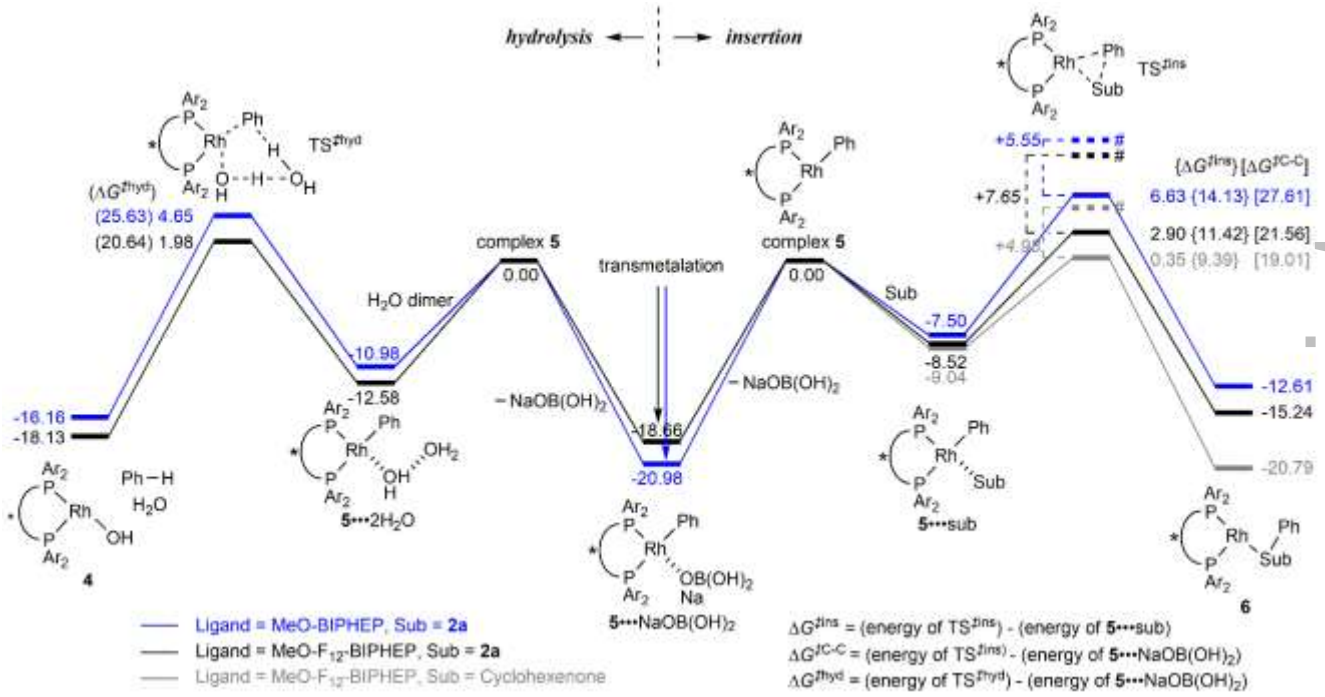

Figure 2. Energy diagrams of insertion or hydrolysis of **5**. Relative Gibss free energies (kcal/mol) obtained by single point energy calculations with the SCRF method based on CPCM (1,4-dioxane) are shown. The energies of $TS^{\neq ins}$ described in plain text were for transition states giving *R*-products. The energies for transition states giving *S*-products were described in italic with dot line and #.

The insertion, or the hydrolysis, of **5** proceeds via $TS^{\neq ins}$, or $TS^{\neq hyd}$, after coordination with the enone substrate (**5•••sub**), or H_2O (**5•••2H$_2$O**) (See Supporting Information, Figure S1). Although the activation energy of insertion had been calculated from the difference between complex **5** and $TS^{\neq ins}$,[29] it is necessary to carefully consider the starting point of insertion step to evaluate the reaction rate. After formation of **5** by transmetalation of PhB(OH)$_2$ (**3a**) to rhodium in the presence of $NaHCO_3$, **5** was stabilized by coordination with NaOB(OH)$_2$ to give complex **5•••**NaOB(OH)$_2$,[30] which was the most stable complex in the **5•••**donating molecules (**2a**, H_2O, 1,4-dioxane, $NaHCO_3$, and NaOB(OH)$_2$) (Scheme 2). The most stable complex **5•••**NaOB(OH)$_2$ would be the mutual short-lived resting-state in both insertion and hydrolysis processes, in other words, the complex is starting point of both insertion and hydrolysis.

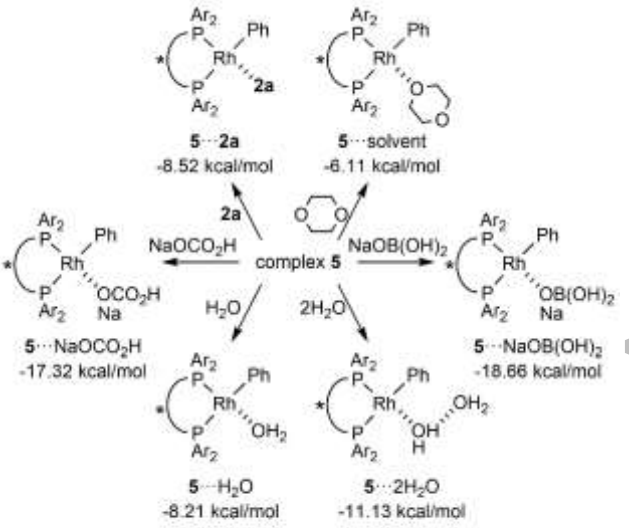

[a]Diphosphine ligand is MeO-F_{12}-BIPHEP. [b]Relative free energies (kcal/mol) obtained by single point energy calculations with the SCRF method based on CPCM (1,4-dioxane) are shown.

Scheme 2. Complex **5** with donating molecules.[a],[b]

This article is protected by copyright. All rights reserved.

Accepted Manuscript

Next, the insertion step was evaluated. Although the activation free energy for insertion ($\Delta G^{\neq ins}$) was evaluated by (energy of $TS^{\neq ins}$) – (energy of **5**•••sub), the k^{ins} would be evaluated using $\Delta G^{\neq C\text{-}C}$ (not $\Delta G^{\neq ins}$) which was calculated by (energy of $TS^{\neq ins}$) – (energy of **5**•••$NaOB(OH)_2$). In the case of MeO-F_{12}-BIPHEP (black in Figure 2), complex **5** was stabilized by $NaOB(OH)_2$ (**5**•••$NaOB(OH)_2$) at -18.66 kcal/mol. The ligand exchange of $NaOB(OH)_2$ to **2a** via unsaturated complex **5** to give **5**•••sub increased the energy level to -8.52 kcal/mol. The insertion proceeded via $TS^{\neq ins}$ to give intermediate complex **6**. The $\Delta G^{\neq ins}$ was 11.42 kcal/mol, and it was larger than the case of highly-reactive cyclohexenone by 2.03 kcal/mol (gray in Figure 2), indicating that substrate **2a** was a less reactive substrate than cyclohexenone. On the contrary, the $\Delta G^{\neq ins}$[MeO-F_{12}-BIPHEP, **2a**] was smaller than that of MeO-BIPHEP by 2.71 kcal/mol, indicating that the electron-poor nature of MeO-F_{12}-BIPHEP accelerated the insertion reaction.[36] Furthermore, in the case of MeO-BIPHEP, more stabilized **5**•••$NaOB(OH)_2$ increased $\Delta G^{\neq C\text{-}C}$, as compared to that of MeO-F_{12}-BIPHEP (27.61 vs. 21.56 kcal/mol). As a result, MeO-BIPHEP was shown to be ineffective for insertion. The energy trends were in agreement with the experimental results in Table 1.

Next, in view of the $\Delta G^{\neq hyd}$, the favorable route for hydrolysis of **5** was the pathway involving bimolecular H_2O (not unimolecular or termolecular H_2O), revealed by the estimation of transition states.[37] In a similar way to $\Delta G^{\neq C\text{-}C}$, $\Delta G^{\neq hyd}$ was calculated by (energy of $TS^{\neq hyd}$) – (energy of **5**•••$NaOB(OH)_2$) to evaluate k^{hyd}. On calculating $\Delta\Delta G^{\neq}$ ($=\Delta G^{\neq C\text{-}C} - \Delta G^{\neq hyd}$) to compare $\Delta G^{\neq C\text{-}C}$ and $\Delta G^{\neq hyd}$ values, the $\Delta\Delta G^{\neq}$ value in the case of MeO-F_{12}-BIPHEP was 0.92 kcal/mol. The result indicates that the insertion reaction is more unfavorable than the hydrolysis of **5**, in agreement with the experimental result (Table 1). Therefore, suppression of the hydrolysis of **5** in a real system would need a negative $\Delta\Delta G^{\neq}$ value obtained by decreasing the $\Delta G^{\neq C\text{-}C}$ or increasing the $\Delta G^{\neq hyd}$ values.

As is evident from the results (Table 1), the introduction of too strong electron-withdrawing groups to the ligand does not lead to an improvement in the reaction yield, and thus, the structures of the $TS^{\neq ins}$ that give the favorable enantiomer were dissected to design the ligand that would decrease the $\Delta\Delta G^{\neq}$ value. The structures of $TS^{\neq ins}$s, bearing (a) (*R*)-MeO-BIPHEP, (b) (*R*)-MeO-F_{12}-BIPHEP, and (c) (*R*)-MeO-3,5-$(CF_3)_2$-BIPHEP, are depicted in Figure 3. Steric (or electronic) repulsion was observed between π-electron of 6-methylcoumarin and lone pair of the *meta*-fluorine on the pendant aryl groups of MeO-F_{12}-BIPHEP, resulting in the aryl group being tilted away from 6-methylcoumarin (D(Rh-P-C^{ipso}-C^{ortho}) = 51.2° for MeO-F_{12}-BIPHEP vs. D(Rh-P-C^{ipso}-C^{ortho}) = 41.4° for MeO-BIPHEP). The larger trifluoromethyl group in MeO-3,5-$(CF_3)_2$-BIPHEP further tilted the aryl group (D(Rh-P-C^{ipso}-C^{ortho}) = 66.8°). In contrast, the attractive CH-π interaction between *ortho*- and *meta*-protons in the pendant phenyl group and the aromatic plane of 6-methylcoumarin was observed in the MeO-BIPHEP system: this was because the C···H distances were 2.69 or 2.73 Å, respectively, which are shorter than sum of their van der Waals radii of C and H (2.9 Å). Although the activation energy for insertion ($\Delta G^{\neq ins}$ or $\Delta G^{\neq C\text{-}C}$) of the MeO-BIPHEP case was larger than that of electron-poor MeO-F_{12}-BIPHEP, the CH-π interaction ought to contribute to the stabilization of its transition state.[7e,38,39] In other words, if such an attractive interaction is introduced into an electron-poor ligand system, it is expected that the activation energy will further decrease.

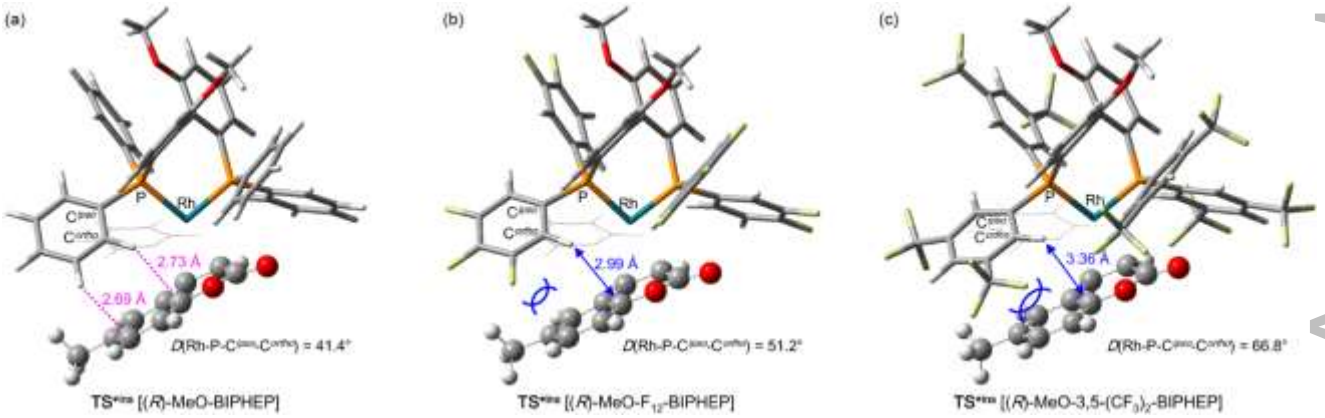

Figure 3. Transition states of insertion of rhodium/(*R*)-ligand with 6-methylcoumarin giving (*R*)-**1aa** as a favorable enantiomer.

We designed chiral ligands **L1**–**L3** for the rhodium-catalyzed 1,4-addition to coumarin substrates (Figure 4). The pendant aryl groups of **L1** (3-fluoro-4-trifluoromethylphenyl group) and **L2** (6-(trifluoromethyl)-3-pyridinyl group), which were inspired by the consideration of the structure of $TS^{\neq ins}$ as mentioned above, have a *meta*-proton in the expectation of a CH–π interaction with the

This article is protected by copyright. All rights reserved.

Accepted Manuscript

coumarin's plane. The both pendant aryl groups for **L1** (σ* = 1.21) and **L2** (σ* = 1.20) show similar electron-withdrawing natures as compared with the 3,4,5-trifluorophenyl group (σ* = 1.11) in MeO-F_{12}-BIPHEP.[40] It should be noted that there are no examples of tertiary phosphines bearing the above asymmetrical fluoroaromatic groups. Among them, no phosphorous compounds bearing the group for **L1** (3-fluoro-4-trifluoromethylphenyl group) had been reported. On the contrary, the pendant aryl of **L3**, 3,5-difluoro-4-trifluoromethyl phenyl group, was chosen by conventional intuition that the electronic poor ligand would accelerate the insertion. The group has no *meta*-proton, but possesses a strong electron-withdrawing ability (σ* = 1.46).[40] The effect of fluorine substituents in pendant aryls on enantioselectivity is expected to cause no problems because all energies of $TS^{\neq ins}$ giving the (*S*)-product in both the MeO-F_{12}-BIPHEP and MeO-BIPHEP cases (dotted line with # in Figure 2) were higher by over 4 kcal/mol than the $TS^{\neq ins}$ giving the (*R*)-product.[41] Before the syntheses of these ligands, the ligand effects on insertion or hydrolysis of **5** were estimated by DFT calculations in a similar manner as mentioned above. The structures of $TS^{\neq ins}$, giving (*R*)-**1aa**, bearing (a) (*R*)-**L1**, (b) (*R*)-**L2**, (c) (*R*)-**L3** are depicted in Figure 5. As expected, the attractive CH–π interaction between the *ortho*- and *meta*-protons in the pendant aryl group and the aromatic plane of the 6-methylcoumarin was observed in both (*R*)-**L1** and (*R*)-**L2** systems, and not observed in the (*R*)-**L3** system.

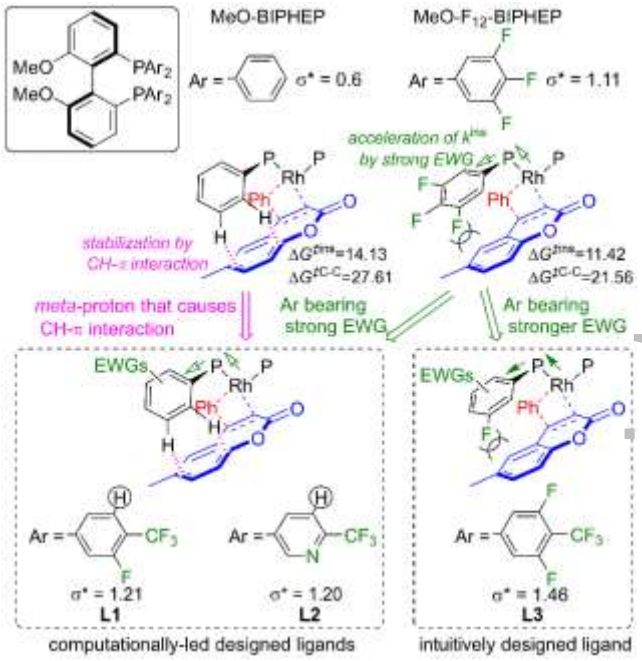

Figure 4. Design of chiral diphosphine ligands bearing fluorofunctional groups.

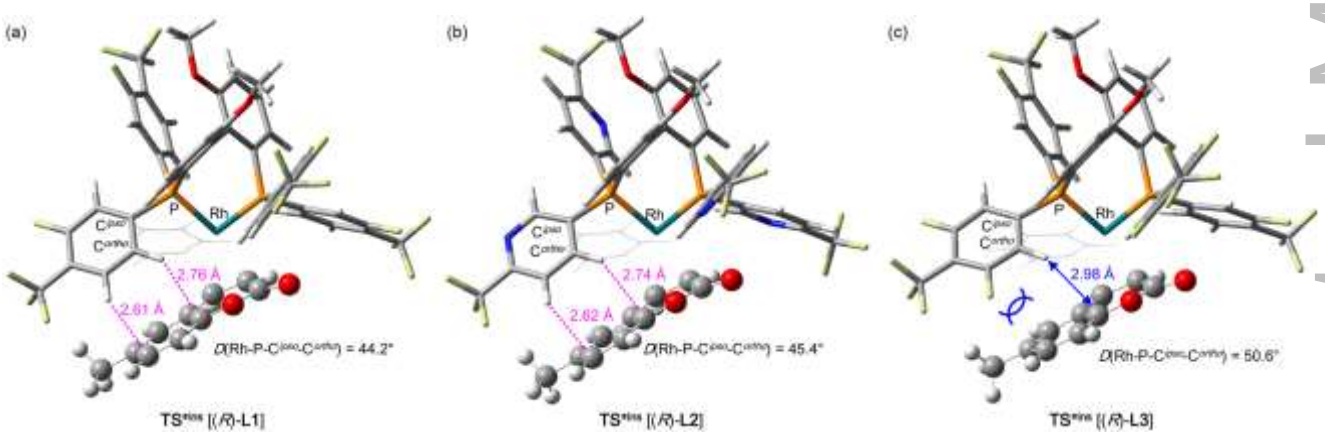

Figure 5. Transition states of insertion of rhodium/designed-ligand with 6-methylcoumarin giving (*R*)-**1aa**.

The $\Delta G^{\neq ins}$, $\Delta G^{\neq C\text{-}C}$, and $\Delta G^{\neq hyd}$ values were calculated in a similar manner to Figure 2 (Table 2). As expected, the $\Delta G^{\neq ins}$ of (*R*)-**L1** or (*R*)-**L2** (10.61 or 11.27 kcal/mol) were lower than that of MeO-F_{12}-BIPHEP system (11.42 kcal/mol). In particular, $\Delta G^{\neq ins}$ of (*R*)-**L1** was decreased by 0.81 kcal/mol from that of MeO-F_{12}-BIPHEP, whose energy difference corresponded to a 3.9-fold acceleration of insertion at 25 °C.[42] It is obvious that the decrease of $\Delta G^{\neq ins}$ is due to the CH–π interaction contribution because rotation of the pendant aryl group of (*R*)-**L1** to the opposite side, (i.e., no CH–π interaction as in the MeO-F_{12}-BIPHEP system) increases the $\Delta G^{\neq ins}$ value to 12.54 kcal/mol (Figure 6)[43]. The stabilization by CH–π interaction of the $TS^{\neq ins}$ giving the (*R*)-product resulted in the expansion of the energy difference from $TS^{\neq ins}$ giving the (*S*)-product by up to 9.07 kcal/mol (Figure 6).

Table 2. Calculation Results for (*R*)-**L1**, (*R*)-**L2**, and (*R*)-**L3**.[a]

Ligand **5**•••$NaOB(OH)_2$	$\Delta G^{\neq ins}$[b]	$\Delta G^{\neq C\text{-}C}$[c]	$\Delta G^{\neq hyd}$[d]	$\Delta\Delta G^{\neq}$[e]
(*R*)-**L1** -18.21	10.61	20.59	21.76	-1.17

This article is protected by copyright. All rights reserved.

Accepted Manuscript

(*R*)-**L2** -17.44	11.27	21.79	23.28	-1.49
(*R*)-**L3** -17.35	11.46	22.24	22.40	-0.16

[a]Relative free energies (kcal/mol) from complex **5** obtained by single point energy calculations with the SCRF method based on CPCM (1,4-dioxane) are shown. [b]$\Delta G^{\neq ins}$ (kcal/mol) = (energy of $TS^{\neq ins}$) – (energy of **5•••2a**). [c]$\Delta G^{\neq C\text{-}C}$ (kcal/mol) = (energy of $TS^{\neq ins}$) – (energy of **5•••**$NaOB(OH)_2$). [d]$\Delta G^{\neq hyd}$ (kcal/mol) = (energy of $TS^{\neq hyd}$) – (energy of **5•••**$NaOB(OH)_2$). [e]$\Delta\Delta G^{\neq} = \Delta G^{\neq C\text{-}C} - \Delta G^{\neq hyd}$.).

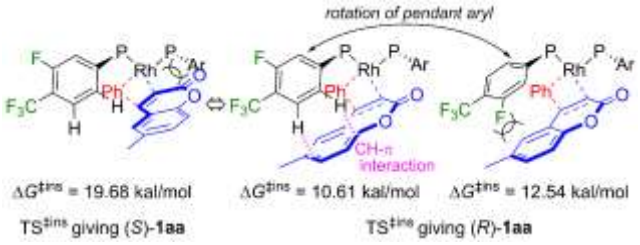

Figure 6. Comparison of $\Delta G^{\neq ins}$ in $TS^{\neq ins}$[(*R*)-**L1**].

The $\Delta G^{\neq C\text{-}C}$ of (*R*)-**L1** (20.59 kcal/mol) also decreased by 0.97 kcal/mol compared to that of MeO-F_{12}-BIPHEP (21.56 kcal/mol), whose energy difference corresponded to a 5.1-fold acceleration of C–C formation at 25 °C.[42] $\Delta G^{\neq hyd}$ of (*R*)-**L1** was increased to 21.76 kcal/mol; therefore, $\Delta\Delta G^{\neq}$ was decreased to -1.17 kcal/mol and the yield of the asymmetric 1,4-addition was expected to improve. On the contrary, the $\Delta G^{\neq C\text{-}C}$ of (*R*)-**L2** (21.79 kcal/mol) did not improve from the case of MeO-F_{12}-BIPHEP. However, the $\Delta G^{\neq hyd}$ of (*R*)-**L2** was increased to 23.28 kcal/mol; therefore, the $\Delta\Delta G^{\neq}$ was decreased to -1.49 kcal/mol beyond the case of (*R*)-**L1**. Although the improvement of the catalytic activity of rhodium/(*R*)-**L2** was not expected, inhibition of hydrolysis of **5** was expected. On the other hand, ligand (*R*)-**L3** was not expected for the asymmetric 1,4-addition because the relatively high $\Delta G^{\neq ins}$ (11.46 kcal/mol) and $\Delta G^{\neq C\text{-}C}$ (22.24 kcal/mol) values would decelerate the insertion step. To conclude the predictions from the computations, good results can be expected by the use of (*R*)-**L1** or (*R*)-**L2**, particularly (*R*)-**L1**, for the asymmetric 1,4-addition of **3a** to **2a**. To test the theoretical predictions, the ligands (*R*)-**L1**, (*R*)-**L2**, and (*R*)-**L3** were synthesized. The ligands were synthesized from known (*R*)-tetrachlorophosphine intermediate **8**, derived from (*R*)-**7** (Scheme 3).[26a] The reaction of (*R*)-**8** with the corresponding Grignard reagents gave the ligands (*R*)-**L1**, (*R*)-**L2**, and (*R*)-**L3** in moderated yields.

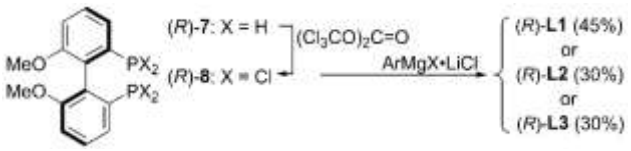

Scheme 3. Syntheses of chiral ligands **L1** – **L3**.

The electronic properties of ligands **L1**, **L2**, and **L3** were estimated using the ν^{CO} values of *cis*-[RhCl(CO)(ligand)] complexes, which were easily synthesized according to the typical method (Table 3).[44] The ν^{CO} values revealed that the electronic properties of the ligands **L1** – **L3** were approximately as expected. The electronic ability of **L1** (2036 cm^{-1}) were identical with MeO-F_{12}-BIPHEP, and that of **L2** were slightly more electron-poor (2038 cm^{-1}). More electron-poor nature of **L3** (2044 cm^{-1}) was equal to MeO-3,5-$(CF_3)_2$-BIPHEP.

Table 3. Electronic Properties of Chiral Ligands[a]

Ligand	ν^{CO} (cm^{-1})
MeO-BIPHEP	2014[b]
MeO-F_{12}-BIPHEP	2036[b]
L1	2036
L2	2038
L3	2044
MeO-3,5-$(CF_3)_2$-BIPHEP	2044[b]

[a]The ν^{CO} values of [RhCl(phosphine)(CO)] in $CHCl_3$. [b]ref. 44.

Similar to the experiments carried out for Table 1 data, asymmetric 1,4-addition reactions of **3a** to **2a** using the ligands **L1** – **L3** were performed (Table 4). As predicted by the calculations described above, ligands (*R*)-**L1** and (*R*)-**L2** improved the yield of (*R*)-**1aa**, and ligand (*R*)-**L3** deteriorated the yield as compared to MeO-F_{12}-BIHEP (entries 1, 9, 10 in Table 4 vs. entry 6 in Table 1). Especially, the yield of the reaction using ligand (*R*)-**L1** was increased up to 53% yield of (*R*)-**1aa** without loss of enantioselectivity (entry 1). The reaction conditions were further investigated by using the most effective (*R*)-**L1** ligand. The yields of (*R*)-**1aa** were influenced by the organic solvent. Although the reactions in Et_2O or CH_2Cl_2 did not progress much (entries 2 or 3), xylene and toluene solvents improved the yields slightly, up to 65%, with >99% ee (entry 4 and 5). Fortunately, toluene is a more suitable solvent for an industrial synthesis than 1,4-dioxane which is a suspected carcinogen.[45] When the amount of **3a** was increased to 3.0 equiv., the yield of (*R*)-**1aa** was over 90% (despite S/C = 2,000) with the longer reaction time of 36 h (entry 6), in contrast with the case using MeO-F_{12}-BIPHEP (Table 1, entry 7). The reaction using 0.033 mol% (S/C = 3,000) or 0.025 mol% (S/C = 4,000) proceeded using 3.5 equiv. **3a** to give 91% or 76% yield of (*R*)-**1aa** with >99% ee, respectively (entries 7 or 8). In view of cost in industrial application, 3.5 equiv. of **3a** would be the maximum value, and S/C =

Accepted Manuscript

This article is protected by copyright. All rights reserved.

2,000 or more is the amount of rhodium catalyst needed to satisfy the requirements for industrial synthesis.[46] Therefore, we judged that the appropriate catalyst and reaction conditions could be discovered.

Table 4. Rhodium-catalyzed Asymmetric 1,4-Addition of **3a** to **2a** using Ligands **L1** – **L3** [a]

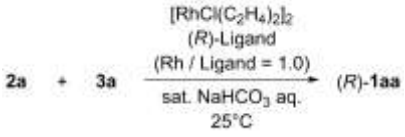

Entry	Ligand	S/C	Solvent	Yield [%]	*ee* [%]	**3a**[b]
1	(*R*)-**L1**	1,000	dioxane	53	>99	none
2	(*R*)-**L1**	1,000	Et_2O	< 1		ca. 90%
3	(*R*)-**L1**	1,000	CH_2Cl_2	6	>99	ca. 90%
4	(*R*)-**L1**	1,000	xylene	60	>99	none
5	(*R*)-**L1**	1,000	toluene	65	>99	none
6[c]	(*R*)-**L1**	2,000	toluene	92	>99	none
7[d]	(*R*)-**L1**	3,000	toluene	91	>99	none
8[e]	(*R*)-**L1**	4,000	toluene	76	>99	none
9	(*R*)-**L2**	1,000	dioxane	33	>99	none
10	(*R*)-**L3**	1,000	dioxane	2	99	ca. 50%

[a]Reaction conditions: **2a** (4.32 mmol), $[RhCl(C_2H_4)_2]_2$ (2.16 μmol, 0.1 mol% of Rh), (*R*)-ligand (4.32 μmol, 0.1 mol%), **3a** (4.32 mmol, 1.0 equiv.) and sat. $NaHCO_3$ (5.8 mL) in organic solvent (4.3 mL) under argon atmosphere at 25 °C for 6 h, unless otherwise specified. [b]Remaining quantity of **3a** was calculated by ^1H NMR. [c]**2a** (4.32 mmol), $[RhCl(C_2H_4)_2]_2$ (1.08 μmol, 0.05 mol% of Rh), (*R*)-**L1** (2.16 μmol, 0.05 mol%), **3a** (13.0 mmol, 3.0 equiv.) and sat. $NaHCO_3$ (5.8 mL) in toluene (4.3 mL) for 36 h. [d]**2a** (6.48 mmol), $[RhCl(C_2H_4)_2]_2$ (1.08 μmol, 0.033 mol% of Rh), (*R*)-**L1** (2.16 μmol, 0.033 mol%), **3a** (22.7 mmol, 3.5 equiv.) and sat. $NaHCO_3$ (8.7 mL) in toluene (6.5 mL) for 48 h. [e]**2a** (8.64 mmol), $[RhCl(C_2H_4)_2]_2$ (1.08 μmol, 0.025 mol% of Rh), (*R*)-**L1** (2.16 μmol, 0.025 mol%), **3a** (30.2 mmol, 3.5 equiv.) and sat. $NaHCO_3$ (11.6 mL) in toluene (8.6 mL) for 60 h.

We carried out the asymmetric 1,4-addition of various coumarin substrates **2** with 3.0 equiv. of arylboronic acids **3** in the presence of 0.05 mol% of rhodium/(*R*)-**L1** catalyst (S/C = 2000) (Table 5). The arylboronic acids bearing electron-donating groups (**3b**–**3d**) gave high to moderate yields of the corresponding (*R*)-**1** with >99% ee (entries 1-3). In contrast, the yield of the reaction with arylboronic acid bearing an electron-withdrawing group (**3e**) was low because decomposition of **3e** was too fast (entry 4). The reaction activity of non-substituted coumarin (**2b**) was similar to that of **2a** (entries 5–7). Although the reactions of 7-methoxycoumarin (**2c**) or 6-ethoxycoumarin (**2d**) with **3a** using conventional ligand had been known to be very less reactive,[17,20] the corresponding products were produced in 73% or 60% yield, respectively (entries 8, 9). However, the reaction of 6-hydroxycoumarin (**2e**) with **3a** did not proceed at all because phenolic hydroxyl groups deactivate the rhodium catalyst.[47]

Table 5. Rhodium-catalyzed Asymmetric 1,4-Addition of Some Coumarin Derivatives using (*R*)-**1**[a]

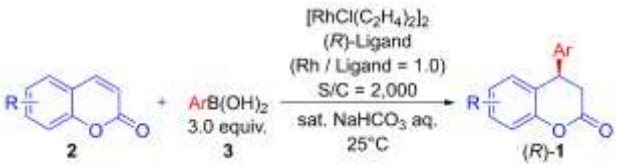

Entry	**2a**	Ar of **3**	Yield [%]	*ee* [%]
1	**2a**	4-Me-C_6H_4 **3b**	71 (*R*)-**1ab**	>99
2	**2a**	3-Me-C_6H_4 **3c**	82 (*R*)-**1ac**	>99
3	**2a**	3,5-Me_2-C_6H_3 **3d**	87 (*R*)-**1ad**	>99
4	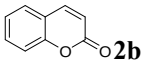 **2b**	4-Cl-C_6H_4 **3e**	25 (*R*)-**1ae**	>99
5	**2b**	**3a**	95 (*R*)-**1ba**	99
6	**2b**	**3b**	76 (*R*)-**1bb**	>99
7	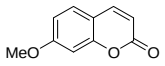 **2c**	**3c**	82 (*R*)-**1bc**	99
8	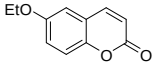 **2d**	**3a**	73 (*R*)-**1ca**	>99
9	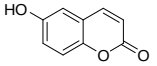 **2e**	**3a**	60 (*R*)-**1da**	>99
10	**2a**	**3a**	0 (*R*)-**1ea**	-

[a]Reaction conditions: **2a** (4.32 mmol), $[RhCl(C_2H_4)_2]_2$ (1.08 μmol, 0.1 mol% of Rh), (*R*)-**L1** (2.16 μmol, 0.1 mol%), **3a** (13.0 mmol, 3.0 equiv.), and sat. $NaHCO_3$ (5.8 mL) in organic solvent (4.3 mL) under argon atmosphere at 25 °C for 36 h.

Although the amount of both the rhodium/(*R*)-**L1** catalyst and **3a** for the catalytic synthesis of (*R*)-**1aa** could be largely reduced, it is important to follow the transformation reaction to a drug molecule for industrial synthesis.[23] Hayashi et al. reported the synthesis of (*R*)-tolterodine as follows: reduction of (*R*)-**1aa**, which was prepared from **2a** with 10 equiv of **3a** in the presence of 3.0 mol% of rhodium/(*R*)-SEGPHOS catalyst in 1,4-dioxane, using

Accepted Manuscript

This article is protected by copyright. All rights reserved.

diisobutylaluminum hydride; followed by 10 mol% of Pd-catalyzed reductive amination with diisopropylamine in MeOH under H_2 atmosphere (50 psi) to produce (*R*)-tolterodine.[17] This method is problematic for industrial application because of the large amounts of rhodium catalyst and **3a** used, but also because of the large amount of palladium catalyst used for reductive amination. The large amount of palladium under a hydrogen atmosphere may increase the danger for a serious accident on the industrial scale. Furthermore, it is desirable for chromatographic purifications to be avoided in the industrial process, particularly silica-gel column chromatography.[17,48] We tried the transformation of (*R*)-**1aa** to (*R*)-tolterodine to 1) avoid using hydrogen gas in a catalytic reductive amination reaction and 2) avoid purification of the synthetic intermediates (Scheme 4). The reduction of 15.07 g (>99% ee) of (*R*)-**1aa** with DIBAL was carried out in a similar manner to ref. 17. After extraction and removal of the organic solvent, crude product **9** was obtained in 16.74 g. The reductive amination of **9** with diisopropylamine without H_2 gas succeeded when using Ir catalyst and HCO_2H. The reaction could be performed using crude product **9** in the presence of only ca. 0.1 mol% of Cp*IrCl[8-quinolinolate] catalyst[49] to give 20.76 g of crude product **10**. According to ^{1}H NMR spectroscopy, after extraction and removal of the organic solvent, the conversion yield of **10** from (*R*)-**1aa** was 70%. Finally, a portion of crude product **10** (1.07 g) without further purification was reacted with (*L*)-tartrate. The generated solid was filtered and washed with cooled EtOH, followed by drying under vacuum to give 0.94 g of pure Detrusitol® ((*R*)-Tolterodine (*L*)-tartrate) with >99% ee. Although the total yield of 60% from (*R*)-**1aa** to Detrusitol® was not very high, the synthetic method -- without using hydrogen gas and without the need of intermediary purification -- will enable large to industrial scale syntheses.

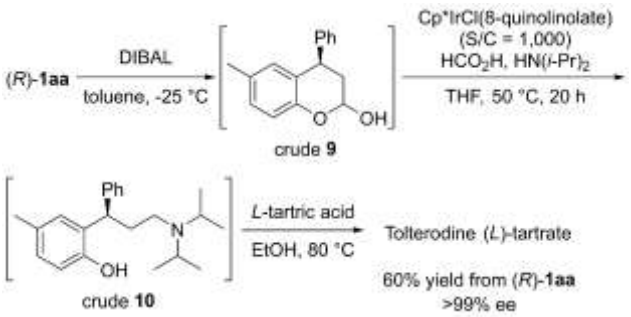

Scheme 4. Gram-scale synthesis of Detrusitol® ((*R*)-tolterodine (*L*)-tartrate) from (*R*)-**1aa**.

Conclusion

In summary, we succeeded in the development of a chiral ligand for the rhodium-catalyzed asymmetric 1,4-addition to a coumarin substrate with low catalyst loading. The ligand was designed through the interplay between theoretical and experimental approaches. The intimate theoretical calculations, including estimation of transition states, were based on experimental results and enabled rational ligand design. The resulting ligand (*R*)-**L1** decreased the catalyst loading of rhodium catalyst to less than one one-hundredth of past catalyst loadings with almost complete enantioselectivity. To our knowledge, this study is the first successful example of drastically decreasing catalyst loading using the interplay between theoretical and experimental approaches. The **L1** could be found out by using the interplay method because the unusual 3-fluoro-4-trifluoromethylphenyl group, which had never been used for the phosphine derivatives, was hard to notice by intuition without computationally assist. We are now trying the computationally-led design method to develop another effective catalyst in a different catalytic system.

Experimental Section

General experimental methods.

All reactions were carried out under an argon atmosphere with dry solvents under anhydrous conditions, unless otherwise noted. All solvents were purchased from Kanto Chemical Co. and then were stored in Schlenk tubes under an argon atmosphere. H_2O was purified by distillation prior to use. Reagents were purchased at the highest commercial quality and used without further purification, unless otherwise noted. Preparative column chromatography was carried out by using silica gel (Kanto Chemical Co. 60N, 63-210 μm). ^{1}H NMR spectra were measured at 400 MHz using tetramethylsilane (TMS) as an internal standard (δ 0 ppm). ^{13}C NMR spectra were measured at 101 MHz, and chemical shifts are given relative to chloroform-*d* (δ 77.16 ppm). ^{19}F NMR spectra were measured at 376 MHz, and chemical shifts are given relative to CCl_3F using C_6F_6 as secondary reference (-162.9 ppm). ^{31}P NMR spectra were measured at 162 MHz, and chemical shifts are given relative to 85% H_3PO_4 externally. IR spectra were measured at resolution 4.0 cm^{-1} or 0.1 cm^{-1} using JASCO FTIR-4200.

Synthesis of (*R*)-(6,6'-dimethoxybiphenyl-2,2'-diyl)bis[bis(3-fluoro-4-trifluoromethylphenyl)phosphine] ((*R*)-L1).

A flame-dried 10 mL screw-cap test tube was flushed with argon and charged with triphosgene (594 mg, 2.0 mmol), was added a solution of Aliquat®336 (47 mg, 0.12 mmol) in toluene (3.3 mL). And then, the solution was stirred at 30 °C for 2 days. To the Schlenk flask containing (*R*)-**7** (278 mg, 1.0 mmol) under argon was added 7.5 mL of dry, deoxygenated CH_2Cl_2 and cooled to -78 °C. After cooling, the solution in screw-cap tube was added to Schlenk flask containing (*R*)-**7** via syringe, and the solution was allowed to warm to r.t. The bright yellow solution was stirred for 2 days. Concentration under vacuum gave the crude (*R*)-**8**. A flame-dried 100 ml three-necked, round-bottomed flask was flushed with argon and charged with magnesium turnings (365 mg, 15.0 mmol), LiCl (317 mg, 7.5 mmol) and 18.3 ml of Et_2O. A solution of DIBAL in hexane (1.0 M, 100 μL, 0.10 mmol) was added and stirred for 5 min. Then 4-bromo-2-fluorobenzotrifluoride (850μL, 6.0 mmol)

Accepted Manuscript

This article is protected by copyright. All rights reserved.

was added and the reaction mixture was stirred for 1 h. Then, a solution of (*R*)-**8** (1.0 mmol) in 1.8 ml of THF was added dropwise over 5 min. The solution was stirred at 40 °C for 4 h, and then saturated aqueous NH_4Cl solution was added. After extracted with EtOAc (three times), the organic layer was dried over Na_2SO_4, filtrated, and concentrated under reduced pressure. The resulting solid was purified by silica gel column chromatography (Hexane/EtOAc = 8/1) to give (*R*)-**L1** as a white solid (413 mg, 0.45 mmol, 45% yield) (See Supporting Information for characterization details).

Syntheses of the **L2** and **L3** were described in Supporting Information

General procedure for rhodium-catalyzed asymmetric 1,4-addition of phenylboronic acid to 6-methylcoumarin.

A 20 mL Schlenk flask was flushed with argon and charged with $[RhCl(C_2H_4)_2]_2$ (0.42 mg, 1.08 μmol, S/C=2,000), (*R*)-**L1** (2.00 mg, 2.16 μmol), and toluene (0.8 mL) was stirred at room temperature for 10 min. This mixture was transferred to a 50 mL Schlenk flask flushed with argon and charged with 6-methylcoumarin (692 mg, 4.32 mmol), $PhB(OH)_2$ (1.58 g, 13.0 mmol), toluene (3.5 mL) and sat. $NaHCO_3$ aq. (5.8 mL) via cannula. The resulting mixture was stirred at 25 °C for 36 h. The reaction mixture was extracted with EtOAc. The organic layer were dried over Na_2SO_4 and concentrated under reduced pressure. The crude material was purified by silica gel column chromatography with hexane/EtOAc = 4 : 1 to give (*R*)-6-methyl-4-phenylchroman-2-one ((*R*)-**1aa**) as a white solid (951 mg, 3.99 mmol, 92% yield, >99% ee) (See Supporting Information for characterization details).

Acknowledgements

This work was supported in part by JSPS KAKENHI (Grant-in Aid for Scientific Research (C), no. 16K05764 (T.K.)) and Grants at Iwate University (T.K.).

References

[1] K. N. Houk, P. H.-Y. Cheong, *Nature* **2008**, *455*, 309-313.

[2] a) D. J. Tantillo, *Acc. Chem. Res.* **2016**, *49*, 1079; b) C. Poree, F. Schoenebeck, *Acc. Chem. Res*. **2017**, 50, 605-608.

[3] a) T. Sperger, I. A. Sanhueza, I. Kalvet, F. Schoenebeck, *Chem. Rev*. **2015**, *115*, 9532-9586; b) X. Zhang, L. W. Chung, Y.-D. Wu, *Acc. Chem. Res.* **2016**, *49*, 1302-1310.

[4] K. Rohmann, M. oelscher, W. Leitner, *J. Am. Chem. Soc.* **2016**, *138*, 433-443.

[5] See *Acc. Chem. Res.* special issue, 2016 "Computational Catalysis for Organic Synthesis".

[6] a) A. S. K. Tsang, I. A. Sanhueza, F. Schoenebeck, *Chem. - Eur. J.* **2014**, *20*, 16432-16441; b) G.-J. Cheng, X. Zhang, L. W. Chung, L. Xu, Y.-D. Wu, *J. Am. Chem. Soc.* **2015**, *137*, 1706-1725.

[7] a) J. C. Ianni, V. Annamalai, P.-W. Phuan, M. Panda, M. C. Kozlowski, *Angew. Chem., Int. Ed.* **2006**, *45*, 5502-5505; b) K. C. Harper, M. S. Sigman, *Science* **2011**, *333*, 1875-1878; c) G. Jindal, R. B. Sunoj, *Org. Biomol. Chem*. **2014**, *12*, 2745-2753; d) B. J. Rooks, M. R. Haas, D. Sepulveda, T. Lu, S. E. Wheeler, *ACS Catal.* **2015**, *5*, 272-280; e) S. E. Wheeler, T. J. Seguin, Y. Guan, A. C. Doney, *Acc. Chem. Res.* **2016**, *49*, 1061-1069; f) A. C. Doney, B. J. Rooks, T. Lu, S. E. Wheeler, *ACS Catal.* **2016**, *6*, 7948-7955; g) J. de Oliveira Silva, R. A. Angnes, V. H. Menezes da Silva, B. M. Servilha, M. Adeel, A. A. C. Braga, A. Aponick, C. R. D. Correia, *J. Org. Chem.* **2016**, *81*, 2010-2018; h) A. J. Neel, A. Milo, M. S. Sigman, F. D. Toste, *J. Am. Chem. Soc.* **2016**, *138*, 3863-3875.

[8] M. C. Nielsen, K. J. Bonney, F. Schoenebeck, *Angew. Chem., Int. Ed*. **2014**, *53*, 5903-5906.

[9] H. Tanaka, Y. Nishibayashi, K. Yoshizawa, *Acc. Chem. Res.* **2016,** *49*, 987-995.

[10] R. N. Straker, Q. Peng, A. Mekareeya, R. S. Paton, E. A. Anderson, *Nature Commun.* **2016**, *7*, 10109.

[11] Y. Takaya, M. Ogasawara, T. Hayashi, M. Sakai, N. Miyaura, *J. Am. Chem. Soc*. **1998**, *120*, 5579-5580.

[12] Recent reviews: a) M. M. Heravi, M. Dehghani, V. Zadsirjan, *Tetrahedron: Asymmetry* **2016**, *27*, 513-588; b) M. Mauduit, O. Basle, H. Clavier, C. Crevisy, A. Denicourt-Nowicki in *Comprehensive Organic Synthesis II*, 2nd ed. (Eds.: P. Knochel, G. A. Molander) Elsevier, Amsterdam, **2014**; Vol. 4, pp 189-341; c) P. Tian, H.-Q. Dong, G.-Q. Lin, *ACS Catal.* **2012**, *2*, 95-119; d) G. Berthon-Gelloz, T. Hayashi in *Boronic Acids*, 2nd ed. (Ed.: D. G. Hall) Wiley-VCH, Weinheim, Germany, **2011**, Vol. 1, pp 263-313; e) G Berthon, T. Hayashi in *Catalytic Asymmetric Conjugate Reactions*, (Ed.: A. Cordova) Wiley-VCH, Weinheim Germany, **2010**, pp 1-70.

[13] a) M. Jean, B. Casanova, S. Gnoatto, P. van de Weghe, *Org. Biomol. Chem.* **2015**, *13*, 9168-9175; b) H. J. Edwards, J. D. Hargrave, S. D. Penrose, C. G. Frost, *Chem. Soc. Rev.* **2010**, *39*, 2093-2105.

[14] J. Magano, J. R. Dunetz, *Chem. Rev.* **2011**, *111*, 2177-2250.

[15] a) J. Magano, J. R. Dunetz in *New Trends in Cross-coupling:Theory and Applications* (Ed.: J. J. Spivey) Royal Society of Chemistry, Cambridge, UK, **2015**, Vol. 21, pp 697-778; b) A. Parker in *Transition Metal-Catalyzed Couplings in Process Chemistry* (Eds.: J. Magano, J. R. Dunetz) Wiley-VCH, Weinheim, Germany, **2013**, pp 121-134; c) G. P. Howell, *Org. Process Res. Dev.* **2012**, *16*, 1258-1272; d) K. Lukin, Q Zhang, M. R. Leanna, *J. Org. Chem*. **2009**, *74*, 929-931; e) S. Brock, D. R. J. Hose, J. D. Moseley, A. J. Parker, I. Patel, A. J. Williams, *Org. Process Res. Dev.* **2008**, *12*, 496-502.

[16] a) Y. Yoshinaga, *J. Pharm. Soc. Japan* **2009**, *129*, 241-245; b) P. Abrams, *Expert opinion on pharm*. **2001**, *2*, 1685-1701.

[17] G. Chen, N. Tokunaga, T. Hayashi, *Org. Lett.* **2005**, *7*, 2285-2288.

Accepted Manuscript

This article is protected by copyright. All rights reserved.

[18] T. Korenaga, R. Maenishi, K. Osaki, T. Sakai, *Heterocycles* **2010,** *80*, 157-162.

[19] Y. Luo, A. J. Carnell, *Angew. Chem., Int. Ed.* **2010**, *49*, 2750-2754.

[20] T. Mino, K. Miura, H. Taguchi, K. Watanabe, M. Sakamoto, *Tetrahedron: Asymmetry* **2015**, *26*, 1065-1068.

[21] C. Defieber, J.-F. Paquin, S. Serna, E. M. Carreira, *Org. Lett.* **2004,** *6*, 3873-3876.

[22] No reaction product was afforded: K. Vandyck, B. Matthys, M. Willen, K. Robeyns, L. Van Meervelt, *Org. Lett.* **2006**, *8*, 363-366.

[23] Problems occurring in a catalytic reaction for industrial scale: C. A. Busacca, D. R. Fandrick, J. J. Song, C. H. Senanayake in *Applications of Transition Metal Catalysis in Drug Discovery and Development* (Eds.: M. L. Crawley, B. M. Troust) John Wiley & Sons, Hoboken, USA, **2012**, pp 1-24.

[24] J.-P. Genet, T. Ayad, V. Ratovelomanana-Vidal, *Chem. Rev.* **2014,** *114*, 2824-2880.

[25] Review for ligand electronic effects in homogeneous catalysis: M. L. Clarke, J. J. R. Frew, *Organomet. Chem.* **2009**, *35*, 19-46.

[26] a) T. Korenaga, K. Osaki, R. Maenishi, T. Sakai, *Org Lett* **2009,** *11*, 2325-2328; b) T. Korenaga, R. Maenishi, K. Hayashi, T. Sakai, *Adv. Synth. Catal.* **2010**, *352*, 3247-3254.

[27] T. Hayashi, M. Takahashi, Y. Takaya, M. Ogasawara, *J. Am. Chem. Soc.* **2002**, *124*, 5052-5058.

[28] The rate-determining step of the reaction using reactive substrate is transmetalation: A. Kina, H. Iwamura, T. Hayashi, *J. Am. Chem. Soc.* **2006**, *128*, 3904-3905.

[29] a) G.-F. Zha, H.-L. Qin, E. A. B. Kantchev, *Org. Biomol. Chem.* **2017**, *15*, 2226-2233; b) J. D. Sieber, D. Rivalti, M. A. Herbage, J. T. Masters, K. R. Fandrick, D. R. Fandrick, N. Haddad, H. Lee, N. K. Yee, B. F. Gupton, C. H. Senanayake, *Org. Chem. Front.* **2016**, *3*, 1149-1153; c) Y.-G. Li, L. Li, M.-Y. Yang, H.-L. Qin, E. A. B. Kantchev, *RSC Adv.* **2015**, *5*, 5250-5255; d) H.-L. Qin, X.-Q. Chen, Y.-Z. Huang, E. A. B. Kantchev, *Chem. - Eur. J.* **2014**, *20*, 12982-12987; e) E. A. B. Kantchev, *Chem. Sci.* **2013**, *4*, 1864-1875; f) S. Gosiewska, J. A. Raskatov, R. Shintani, T. Hayashi, J. M. Brown, *Chem. - Eur. J.* **2012**, *18*, 80-84; g) E. A. B. Kantchev, *Chem. Commun.* **2011**, *47*, 10969-10971; h) A. Poater, F. Ragone, R. Mariz, R. Dorta, L. Cavallo, *Chem. - Eur. J.* **2010**, *16*, 14348-14353; i) P. Mauleon, I. Alonso, M. Rodriguez Rivero, J. C. Carretero, *J. Org. Chem.* **2007**, *72*, 9924-9935; j) T. Itoh, T. Mase, T. Nishikata, T. Iyama, H. Tachikawa, Y. Kobayashi, Y. Yamamoto, N. Miyaura, *Tetrahedron* **2006**, *62*, 9610-9621.

[30] Evaluation of transmetalation as a rate determining step by DFT calculations: a) ref. 29a. b) Y.-G. Li, G. He, H.-L. Qin, E. A. B. Kantchev, *Dalton Trans.* **2015**, *44*, 2737-2746.

[31] S. Grimme, *J. Comput. Chem*. **2006**, *27*, 1787-1799.

[32] For Gaussian basis sets: a) M. J. Frisch, J. A. Pople, J. S. Binkley, *J. Chem. Phys*. **1984**, *80*, 3265-3269; b) W. J. Hehre, L. Radom, P. v. R. Schleyer, J. A. Pople in *Ab initio Molecular Orbital Theory*; John Wiley: New York, USA, **1986** , and references cited therein.

[33] Gaussian 09, Revision E.01; Gaussian, Inc., Wallingford, CT, 2009.

[34] V. Barone, M. Cossi, *J. Phys. Chem. A* **1998**, *102*, 1995-2001.

[35] Transition states in insertion step of Rh-diphosphine complexes: see refs. 29d, 29h, 29i, 29j.

[36] Q. Chen, B.-L. Lin, Y. Fu, L. Liu, Q.-X. Guo, *Res. Chem. Intermed.* **2005**, *31*, 759-767.

[37] $\Delta G^{\neq hyd}(2H_2O)$ = 20.64 kcal/mol *vs*. $\Delta G^{\neq hyd}(H_2O)$ = 23.24 kcal/mol or $\Delta G^{\neq hyd}(3H_2O)$ = 21.08 kcal/mol in the cases of MeO-F_{12}-BIPHEP. See Figure S1 in Supporting Information.

[38] a) A. J. Neel, M. J. Hilton, M. S. Sigman, F. D. Toste, *Nature* **2017**, *543*, 637-646; b) E. H. Krenske, K. N. Houk, *Acc. Chem. Res.* **2013**, *46*, 979-989.

[39] The B97D functionals afforded good results for consideration of CH-π interaction: S. Tsuzuki, *Annu. Rep. Prog. Chem., Sect. C: Phys. Chem.* **2012**, *108*, 69-95.

[40] Taft's σ* values were evaluated according to the following reference: Y. Nagai, H. Matsumoto, T. Nakano, H. Watanabe, *Bull. Chem. Soc. Jap.* **1972**, *45*, 2560-2565.

[41] The energy difference by 3.1 kcal/mol is a value that corresponds to the experimentally measured 99% ee at 25 °C.

[42] The ratio of reaction rate was calculated by equation of $e^{(\Delta G\neq[\text{MeO-F12-BIPHEP}]-\Delta G\neq[\mathbf{L1}])/RT}$.

[43] In the calculations of **L2**, similar results were obtained. See Figure S2 in supporting information.

[44] T. Korenaga, A. Ko, K. Uotani, Y. Tanaka, T. Sakai, *Angew. Chem. Int Ed Engl* **2011**, *50*, 10703-10707.

[45] U.S. Environmental Protection Agency. Integrated Risk Information System (IRIS). 1,4-Dioxane (CASRN 123-91-1), **2013**.

[46] S. Huebner, J. G. de Vries, V. Farina, *Adv. Synth. Catal.* **2016**, *358*, 3-25.

[47] F.-X. Chen, A. Kina, T. Hayashi, *Org. Lett.* **2006**, *8*, 341-344.

[48] Separation processes account for 40−70% of both capital and operating costs in the chemical and pharmaceutical industries: P. Marchetti, M. F. Jimenez Solomon, G. Szekely, A. G. Livingston, *Chem. Rev.* **2014**, *114*, 10735-10806, and references therein.

Accepted Manuscript

This article is protected by copyright. All rights reserved.

10.1002/adsc.201701191

[49] a) M. Watanabe, J. Hori, K. Murata, Patent JP5719115, **2015**; b) M. Watanabe, J. Hori, K. Murata, Patent EP2228377, **2014**; c) M. Watanabe, J. Hori, K. Murata, Patent US9211533, **2015**.

Accepted Manuscript

This article is protected by copyright. All rights reserved.

10.1002/adsc.201701191

FULL PAPER

Computationally-led Ligand Modification using Interplay between Theory and Experiments: Highly Active Chiral Rhodium Catalyst Controlled by Electronic Effects and CH–π Interactions

Adv. Synth. Catal. **Year**, *Volume*, Page – Page

Toshinobu Korenaga,* Ryo Sasaki, Toshihide Takemoto, Toshihisa Yasuda, Masahito Watanabe

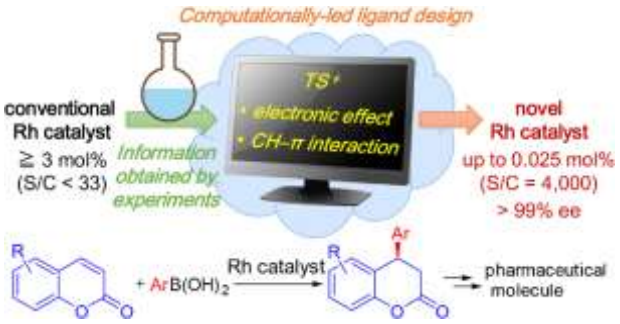

Accepted Manuscript

This article is protected by copyright. All rights reserved.